

Distribution of reflection coefficients in absorbing chaotic microwave cavities

R. A. Méndez-Sánchez,¹ U. Kuhl,² M. Barth,² C. H. Lewenkopf,³ and H.-J. Stöckmann²

¹*Centro de Ciencias Físicas UNAM, A.P 48-3, 62210, Cuernavaca, Morelos, México*

²*Fachbereich Physik, Philipps-Universität Marburg, Renthof 5, D-35032 Marburg, Germany*

³*Instituto de Física, UERJ, R. São Francisco Xavier 524, 20550-900 Rio de Janeiro, Brazil*

(Dated: February 7, 2020)

The distribution of reflection coefficients $P(R)$ for chaotic microwave cavities with time-reversal symmetry is investigated in different absorption and antenna coupling regimes. For all regimes the agreement between experimental distributions and random-matrix theory predictions is very good, provided both the antenna coupling T_a and the wall absorption strength T_w are taken into account in an appropriate way. These parameters are determined by independent experimental quantities.

PACS numbers: 42.25.Bs, 03.65.Nk, 73.23.-b, 05.60.-k

Wave scattering by chaotic and weak disordered systems has motivated a rather intensive research activity. The subject is common to several areas of physics, ranging from nuclear, atomic, molecular, and mesoscopic physics to classical wave scattering, like microwaves, sound, and light (see Refs. [1, 2] for a review). The striking feature shared by all such systems, provided they have a chaotic underlying classical dynamics, is that they show universal transmission fluctuations. These fluctuations are successfully described by random-matrix theory [3, 4]. Very recently a comprehensive treatment of absorption, ubiquitous in experiments, was developed for systems without time-reversal symmetry (TRI) [5, 6]. For systems with TRI, however, there is a rigorous theory only in limiting cases [5].

An analytical expression for the distribution $P(R)$ of the reflection coefficient R in the presence of absorption was derived for an arbitrary number of open channels in the weak absorption limit [7]. In the strong absorption limit $P(R)$ reduces to a simple exponential [8]. In these two works perfect coupling between the channels and the scattering region is assumed. Furthermore, non-resonant backscattering processes [9, 10, 11], which are present in most experimental situations, have been until now often neglected in cases that absorption is taken into account. It is noteworthy that only few of these works are experimental [12, 13, 14].

The purpose of this letter is to present experimental evidence that random-matrix theory provides a quantitative understanding of the universal reflection fluctuations in chaotic systems. More specifically, we show that this can only be achieved if both the coupling, so far mostly overlooked, and absorption strengths are properly taken into account. To this end we measure $P(R)$ in microwave cavities from weak to strong absorption regimes. A quantitative agreement between experiment and theory is observed for all the cases we have studied. This is remarkable since all theoretical parameters are directly obtained from averaged experimental quantities and not from a fit of $P(R)$ to the data.

To study the dependence of $P(R)$ on absorption and

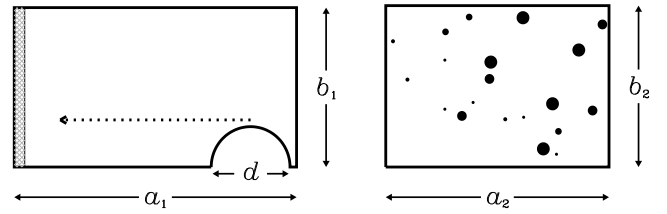


FIG. 1: Sketch of the microwave billiards. (left) Half Sinai billiard ($a_1 = 43$ cm, $b_1 = 23.7$ cm, height $h_1 = 7.8$ mm). The half disk ($d = 12$ cm) was moved along a_1 . For the second set of measurements one wall was coated with an absorber. (right) Disordered billiard ($a_2 = 34$ cm, $b_2 = 24$ cm, height $h_2 = 8$ mm) [16]. The billiards are drawn at scale.

coupling strengths, we used three different flat microwave cavities and measured the reflection. For the half Sinai billiard, Fig. 1(left), 57 reflection spectra were measured by sliding the half circular inset along the wall over 28.5 cm in steps of 0.5 cm. This is a practical way to improve the statistics, notwithstanding the correlations among spectra. For all cases only one antenna is coupled to the cavity. For the second measurement, one wall of the half Sinai billiard was coated with an absorber [15]. The third measurement was performed on a disordered billiard [16], where 20 brass cylinders of 5 different sizes have been located at random within the billiard (Fig. 1(right)). The data were collected on a 5 mm grid with 696 antenna positions. We do not consider antenna positions closer than 15 mm to the billiard walls, so only 533 measurements are included in the statistical analysis. The reflection coefficients R were measured with vector network analyzers. Typical absorption spectra for the three cases are shown in Fig. 2.

Figure 3 shows the mean reflection coefficient $\langle R \rangle$ as a function of the frequency ν for the different cavities. $\langle \dots \rangle$ denotes averaging over a frequency range $\Delta\nu$ (see Fig. 3 and over different cavity geometries (half Sinai billiard) or different antenna positions (disordered billiard)). Five representative windows, where $\langle R \rangle$ is approximately constant, are chosen for a detailed statistical investigation. The windows correspond to the shaded areas in Fig. 3.

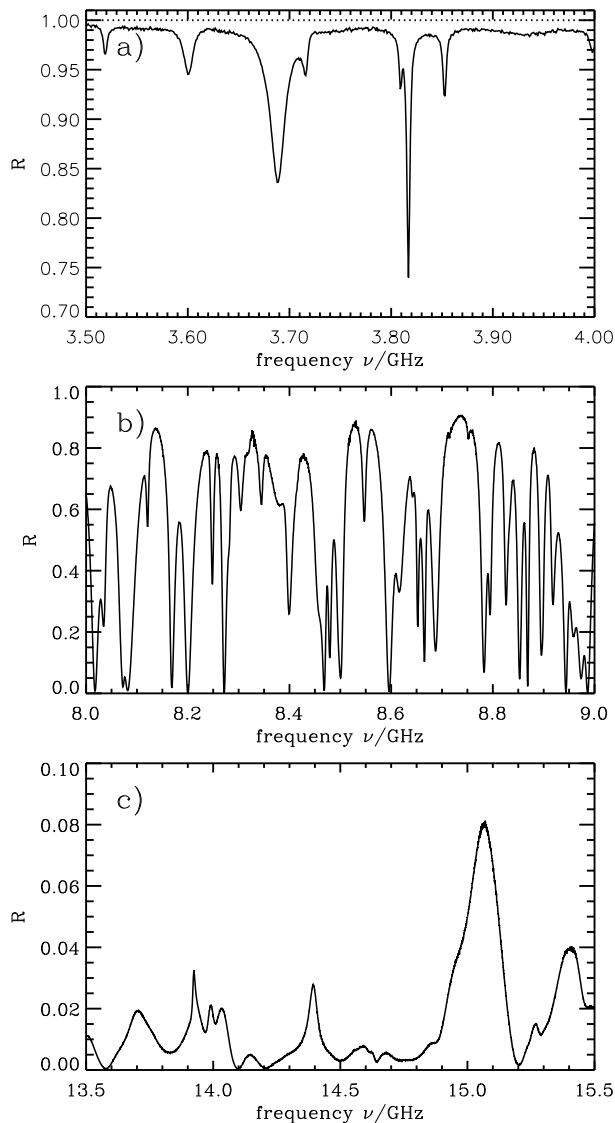


FIG. 2: Typical absorption spectra for different absorption regimes: (a) Weak absorption and weak coupling - disordered billiard, (b) intermediate absorption and coupling - half Sinai billiard, and (c) strong absorption and perfect coupling - half Sinai billiard with absorber.

We shall now discuss how $P(R)$ is obtained using random-matrix theory [1]. The scattering matrix S is unitary and has a dimension N , the number of open channels. Since absorption opens new channels, the experimentally accessible N_{exp} -channel sector of S , which we call \tilde{S} , becomes subunitary. As a result, the eigenvalues $R_1, R_2, \dots, R_{N_{\text{exp}}}$ of $\tilde{S}\tilde{S}^\dagger$ lie between 0 and 1 [7]. In the whole frequency range the diameter of the antenna is small compared to the wavelength implying a single coupled channel, i. e., there is a single measurable reflection coefficient R . The resonant S matrix for quantum systems [17] can be used to describe cavity microwave

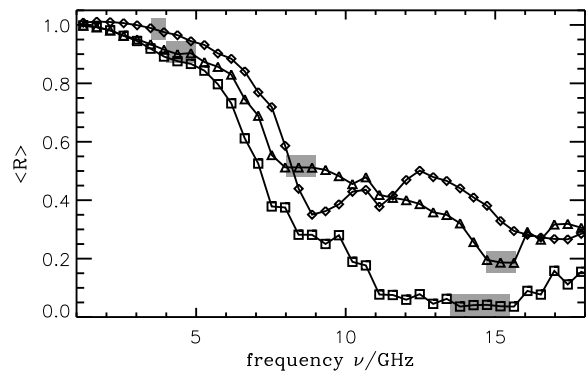


FIG. 3: Average reflection $\langle R \rangle$ as a function of the frequency ν for: half Sinai (triangles), half Sinai with absorber (squares) and disordered (diamonds), cavities. The shaded boxes mark the cases subjected to a detailed analysis. The frequency average is $\Delta\nu=450$ MHz.

scattering [18, 19], and reads

$$S(E) = 1 - 2\pi i W^\dagger (E - H + i\pi W W^\dagger)^{-1} W. \quad (1)$$

The quantum mechanical energy E is related to the electromagnetic frequency ν by Weyl's formula. In the high-frequency limit $E \sim \nu^2$, whereas at low frequencies the dispersion relation depends on the cavity shape. H describes the cavity quasi-bound spectrum, and W contains the coupling matrix elements between the resonances and the scattering channels. These are the absorption channels in the cavity $N_w \gg 1$ and the microwave antenna $N_a = 1$ [18]. These absorption channels act as additional “fictitious” waveguides attached to the cavity [20].

In our statistical treatment we take the matrix H as being a member of the Gaussian orthogonal ensemble, as usual for time-reversal invariant chaotic systems. Since the H matrix is statistically invariant under orthogonal transformations, the statistical properties of S depend only on the mean resonance spacing Δ (determined by H) and on the traces of $W^\dagger W$. The average scattering properties are best characterized by the transmission coefficients of the antenna t_a and of the fictitious waveguides t_w . These coefficients are defined as $t_c = 1 - |\overline{S_{cc}}|^2$, where c is an arbitrary channel and $\overline{\dots}$ stands for an ensemble average. The ergodic hypothesis identifies the later with the experimental frequency averages. Weak coupling corresponds to $t_c \rightarrow 0$, or direct reflection from channel c (no flux entering the cavity), whereas $t_c \rightarrow 1$ is the limit of perfect coupling. Hence, our model has two parameters, namely, the antenna coupling $T_a = t_a$ and the absorption strength $T_w = N_w t_w$.

Analytical results for $P(R)$ in the case of time-reversal invariant systems are known only for the limiting cases of very weak ($T_w \ll 1$) or strong absorption ($T_w \gg 1$) with perfect antenna coupling ($T_a = 1$). For most cases of interest one has to rely on numerical simulations of the resonant S matrix as given by Eq. (1). This is done

billiard	$\Delta\nu/\text{GHz}$	$\langle R \rangle$	T_a	T_w
disordered	3.5- 4.0	0.981	0.011	0.49
half Sinai	4.0- 5.0	0.906	0.116	0.56
half Sinai	8.0- 9.0	0.517	0.754	2.42
half Sinai	14.7-15.7	0.185	0.989	8.40
absorbing wall	13.5-15.5	0.039	0.998	48.00

TABLE I: Mean reflection coefficient $\langle R \rangle$, antenna coupling T_a , and wall absorption T_w for the cases marked in Fig. 3. $\Delta\nu$ is the frequency range.

as follows: first, T_a and T_w determine W [17]; second, by picking H from the Gaussian orthogonal ensemble we compute S . In this study we generate 10^5 realizations of H with dimension $M = 201$ and fix $N_w = 200$ for each case of interest. These values are justified as follows: The exact value of N_w is not of relevance, provided $N_w \gg 1$, as demonstrated in Ref. [21]. The statistical theory requires $M \gg 1$, which is the case in our experiment. Finally, for technical reasons $M > N_w$ [17].

The transmission coefficients T_a and T_w are obtained directly from the experimental data as follows: First, we use $t_a = 1 - \langle |S_{aa}|^2 \rangle$ to determine T_a directly from the measured values of $S_{aa}(\nu)$. T_w is then fixed by adjusting the theoretical mean reflection coefficient $\langle R \rangle$ to the experimental one. In the low frequency regime, the values of $\langle S_{aa}(\nu) \rangle$ and $\langle R \rangle$ cannot be extracted correctly from the experimental data since the background of the reflection spectrum varies slowly with ν and deviates from unity, as shown in Fig. 2(a). These variations of the background cause a broadening of the distribution and a shift of its maximum. This problem can be overcome as follows: Since in this regime the resonances are nearly isolated, each of them can be fitted by a complex Lorentzian. Using these fits a corrected spectrum can be generated with a perfect background and suppression of noise. From this spectrum $\langle S_{aa} \rangle$, $\langle R \rangle$, and $P(R)$ are obtained. The values for the mean reflection coefficient $\langle R \rangle$, the antenna transmission T_a , and the wall absorption T_w for the five regions under investigation are shown in Table I.

We first discuss the regime of strong absorption. The theoretical distribution is given by [8]

$$P(R) = \langle R \rangle^{-1} e^{-R/\langle R \rangle}, \quad (2)$$

which no longer depends explicitly on the number of open channels. Experimentally, the system with the largest absorption is the half Sinai billiard with absorber as seen in Fig. 3. A typical spectrum is presented in Fig. 2(c). The corresponding experimental distribution $P(R)$ is shown in Fig. 4, together with the prediction of Eq. (2) and the numerical simulation. The theory contains no free parameters since the only inputs, namely T_a and $\langle R \rangle$, were independently extracted from the experimental data. A strong variation of T_w in the investigated

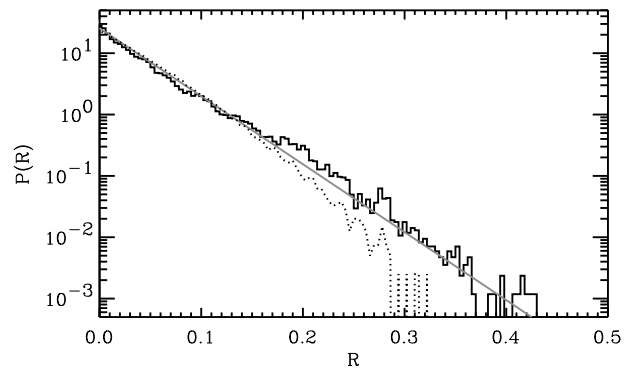


FIG. 4: Distribution of the reflection coefficient R for the half Sinai billiard in the strong absorption limit (13.5-15.5 GHz). The solid line corresponds to Eq. (2) and the dotted one to the numerical simulation.

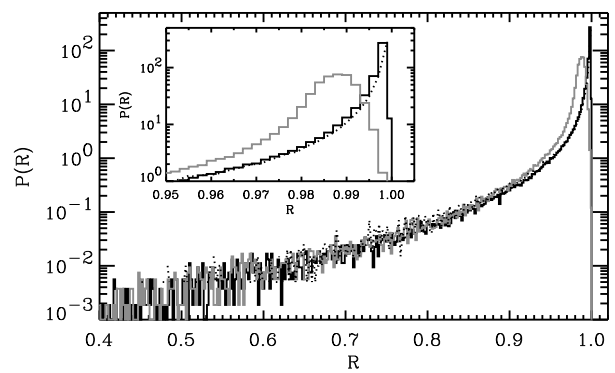


FIG. 5: Distribution of the reflection coefficients, $P(R)$, for weak coupling strength and small absorption (3.5-4.0 GHz), obtained from the Lorentzian fit corrected spectrum (for details see text). For comparison the distribution obtained from the uncorrected spectrum is shown in light grey. The inset enlarges the region of R between 0.95 and 1.005. The dotted line is obtained from the random-matrix simulation.

frequency range causes the discrepancy between the experiment and the simulation.

Let us now turn to the weak absorption regime, $T_w < 1$, at low frequencies. Unfortunately, the available analytical result [7] cannot be used, since it assumes perfect coupling, whereas in the present experiment, the coupling is weak at low frequencies (see Table I). A similar distribution for nearly perfect coupling has been presented in Ref. [12], but no detailed analysis is performed. In Fig. 5 the distribution of $P(R)$ is shown for the disordered cavity in the frequency region of 3.5 to 4.0 GHz, obtained from the Lorentzian-fit corrected-spectra. This is beyond the localization-delocalization transition observed at about 3 GHz for the disordered cavity of Fig. 1(right) (a selection of eigenfunctions can be found in Ref. [16]). The results from the numerical simulation are plotted for comparison with almost perfect agreement.

The experimental distributions $P(R)$ for intermediate

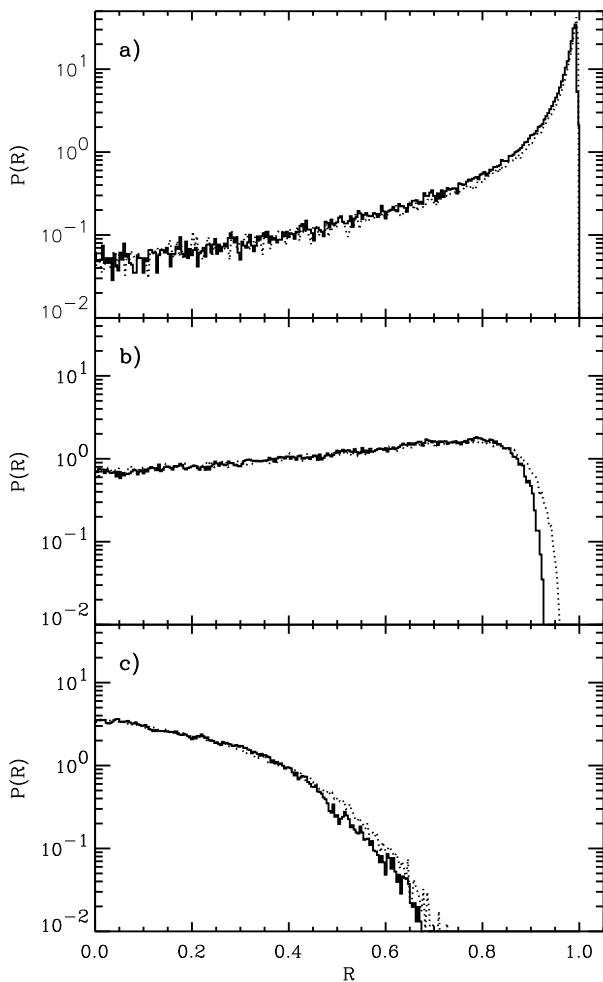


FIG. 6: Distribution of the reflection coefficients $P(R)$ for the intermediate absorption regime (half Sinai billiard). The data were collected at different frequency windows marked in Fig. 3. The dashed lines stand for the random-matrix simulations. In (a) the experimental distribution was obtained from the Lorentzian fit corrected spectrum.

absorption and coupling regimes are presented in Fig. 6. The data are taken from the half Sinai billiard depicted in Fig. 1(left). A typical spectrum for the intermediate regime is shown in Fig. 2(b). In all cases, a very good agreement between the experimental and theoretical $P(R)$ is found.

It was essential to extract the coupling and the absorption strength from two independent experimental quantities. The coupling strength depends on the phase variations of S through $\langle S \rangle$, whereas the absorption strength depends on the average $\langle R \rangle$. We obtain a good agreement between experiment and theory, comparable to the one displayed in Fig. 6, by assuming perfect coupling ($T_a = 1$) and thus overestimating the absorption. Such agreement can lead to a wrong understanding of the actual physical process at hand. This is an important message to bear in mind when analyzing quantum mechanical processes, where in most cases the phase of S cannot be measured.

We have shown that microwave experiments with chaotic and disordered billiards are excellent tools to investigate the universal distribution of reflection coefficients with absorption. We studied a broad variety of regimes, ranging from weak coupling and weak absorption to perfect coupling and strong absorption. In all cases a very good agreement between experiment and theory was found. This is particularly striking, since the theoretical input parameters were fixed independently by the experiment.

We thank C. W. J. Beenakker, P. A. Mello, O. Legrand, J. Flores, and R. Schäfer for helpful conversations and T. H. Seligman and Centro Internacional de Ciencias (Cuernavaca) for hospitality. This work was supported by DGAPA-UNAM, CONACyT (México), CNPq (Brazil), and the DFG (Germany).

-
- [1] C. W. J. Beenakker, *Rev. Mod. Phys.* **69**, 731 (1997).
 - [2] H.J. Stöckmann, *Quantum Chaos*, (Cambridge University Press, Cambridge, 1999).
 - [3] T.A. Brody, J. Flores, J. B. French, P. A. Mello, A. Pandey, and S.S.M. Wong, *Rev. Mod. Phys.* **53**, 385 (1981).
 - [4] T. Guhr, A. Müller-Groeling, and H. A. Weidenmüller, *Phys. Rep.* **299**, 189 (1998).
 - [5] D.V. Savin and H.-J. Sommers, cond-mat/0303083.
 - [6] Y.V. Fyodorov, cond-mat/0304671.
 - [7] C.W.J. Beenakker and P.W. Brouwer, *Physica E* **9**, 463 (2001).
 - [8] E. Kogan, P.A. Mello, and He Liqun, *Phys. Rev. E* **61**, R17 (2000).
 - [9] P.W. Brouwer and C.W.J. Beenakker, *Phys. Rev. B* **50**, 11263 (1994).
 - [10] P.W. Brouwer, *Phys. Rev. B* **51**, 16878 (1995).
 - [11] V.A. Gopar and P.A. Mello, *Europhys. Lett.* **42**, 131 (1998).
 - [12] E. Doron, U. Smilansky, and A. Frenkel, *Phys. Rev. Lett.* **65**, 3072 (1990).
 - [13] M. Stoytchev and A.Z. Genack, *Phys. Rev. Lett.* **79**, 309 (1997).
 - [14] H. Schanze, E. R. P. Alves, C. H. Lewenkopf, and H.-J. Stöckmann, *Phys. Rev. E* **64**, 065201(R) (2001).
 - [15] The absorber is a carbon loaded polyurethane foam of 5cm width and an absorption larger than 20dB in the frequency range we have used.
 - [16] H.-J. Stöckmann *et al.*, *Physica E* **9**, 571 (2001).
 - [17] J. J. M. Verbaarschot, H. A. Weidenmüller, and M. R. Zirnbauer, *Phys. Rep.* **129**, 367 (1985).
 - [18] C. H. Lewenkopf, A. Müller, and E. Doron, *Phys. Rev. A* **45**, 2635 (1992).
 - [19] Y.V. Fyodorov and H.-J. Sommers, *J. Math. Phys.* **38**, 1918 (1997).
 - [20] The channels in Eq. (1) are defined in the Hilbert space. Hence the “fictitious” channels can, in principle, model wall as well as bulk absorption.
 - [21] R. Schäfer, T. Gorin, T.H. Seligman, and H.-J. Stöckmann, *J. Phys. A* **36**, 3289 (2003).